Journal of Applied Polymer Science

# Thermal, mechanical, and rheological properties of graphite- and graphene oxide-filled biodegradable polylactide/poly(ε-caprolactone) blend composites

**Orebotse Joseph Botlhoko,[1,2] James Ramontja,[1] Suprakas Sinha Ray [1,2]**

[1]Department of Applied Chemistry, University of Johannesburg, Doornfontein 2028, Johannesburg, South Africa

[2]DST-CSIR National Centre for Nano-structured Materials, Council for Scientific and Industrial Research, Pretoria 0001, South Africa

Correspondence to: S. S. Ray (E-mail: rsuprakas@csir.co.za or suprakas73@yahoo.com)

**ABSTRACT:** The effect of graphite (G) and graphene oxide (GO) dispersions on the thermal, mechanical, rheological properties of biodegradable polylactide (PLA)/poly(ε-caprolactone) (PCL) blend composites has been comparatively investigated. Surface morphology analysis indicates that the degree of morphological stability depends on not only the loading of the filler but also enthalpic interaction between the filler surface and the polymer blend. A significant improvement in the elongation at break (43.8%), with well-balance of modulus and strength characteristics, is observed for the G-filled (0.25 wt %) blend composite, whereas the GO-filled (0.05 wt %) ternary composite shows a strong (~19 °C) improvement in the thermal stability. Furthermore, the dynamic modulus of the blends increased after composite formation; however, the degree of improvement is greater for the G-filled blend composites. On the basis of the obtained results, we propose a general description of how the morphology and structure of the blend composites are related to the final properties. © 2017 Wiley Periodicals, Inc. J. Appl. Polym. Sci. **2017**, *134*, 45373.

**KEYWORDS:** biodegradable; graphene and fullerenes; mechanical properties; rheology; thermal properties

Received 14 March 2017; accepted 18 May 2017

**DOI: 10.1002/app.45373**

## INTRODUCTION

Polylactide (PLA) is aliphatic polyester that is produced by conversion of corn, sugarcane, etc., followed by fermentation into lactic acid (LA), purification, and finally polymerization of the LA into PLA.[1–3] PLA is obtained from renewable resources, is highly biocompatible, has good mechanical properties, and yields transparent processed materials. However, its brittleness and low melt strength limit its practical application.[4] For this reason, there is growing research interest in making PLA more flexible without losing its inherent stiffness and material properties. To this end, various soft biodegradable polymers, such as poly(ε-caprolactone) (PCL), poly(glycolide), poly(butylene succinate), and poly(butylene succinate-*co*-adipate), have been blended with PLA to reduce its brittleness.

In this study, PCL was selected to reduce the brittleness of PLA in order to form an interesting material that may be used for different industrial applications in the future. In general, the final properties of immiscible PLA/PCL blends are strongly influenced by the morphology of the system, such as the size of the dispersed droplet phase and the interface.[5] In recent years, to stabilize the immiscible blend morphology in order to obtain desired properties, the use of various types of solid particles as morphological stabilizers has received much attention owing to their large specific area per unit volume and lower cost compared with available copolymer compatibilizers.[6,7] In such particles-filled blends, particles could be preferentially localized in either of the two matrices or at the interface, leading to a thermodynamically favorable morphology and hence improved mechanical and material properties. Preferential localization of solid particles is driven mainly by two factors: first, enthalpic interaction between each phase and the solid particles and second, the viscosity ratios of the two polymer matrices. Solid particles that are commonly used for this purpose include nanoclay, carbon nanotubes, graphene oxide (GO), magnesium oxide, titanium oxide, and silica.[6–9]

For example, Mofokeng and Luyt[10] reported blending PLA with PCL reduced the thermal stability of both individual polymers; however, introducing $TiO_2$ nanoparticles (NPs) increased the thermal stability of the blends. Transmission electron microscopy (TEM) study revealed that most of the $TiO_2$ NPs were

Additional Supporting Information may be found in the online version of this article.

located in the PLA phase. Eng *et al.*[11] reported on the mechanical and thermal properties of Nanomer PGV (a hydrophilic nanoclay)- and MMTK10-modified PLA/PCL blends. The addition of Nanomer PGV significantly improved the flexibility of the blends and slightly shifted the glass transition temperature ($T_g$) of the blends. They attributed this result to the compatibilization effect of Nanomer PGV. On the other hand, the addition of MMTK10 made the blends stiffer. In addition, the introduction of nanoclay improved the thermal stability of the blends. However, TEM images revealed the formation of agglomerates in the composites. Liang *et al.*[12] reported the tensile properties of PLA/PCL/$CaCO_3$ composites; they performed experiments at different PCL loadings and also at different strain rates with a constant PCL content. They found that the tensile properties increased slightly with increasing strain rate at a constant PCL loading. However, nonlinear degradation of the tensile properties was observed with increasing PCL content. Recently, Agwuncha *et al.*[13] reported significant improvement in the elongation at break when they modified PLA/PCL blends with 4 wt % boehmite NPs. Morphological analysis using TEM revealed partial compatibilization between phases in the presence of boehmite NPs.

Recently, GO particles have been extensively used to prepare polymer composites with improved mechanical and material properties.[9,14] GO is a well-known carbon-based nanomaterial and is produced through oxidation of inexpensive graphite (G) powder in strong acid media or ozone or by chemical/thermal exfoliation of graphite oxide.[15] GO is a two-dimensional amphiphilic material made of loosely bound layers of carbon atoms in an arrangement structurally similar to that of a graphene sheet. Specifically, GO consists of a graphene sheet decorated with phenyl epoxide and hydroxyl groups on the basal plane and carboxylic acid groups on the edges.[16,17] Because GO has the graphene structure, it also has properties similar to those of graphene, such as superior mechanical properties, optical properties, and electronic conductivity. Furthermore, it is one of the thinnest, strongest, and stiffest materials in the world, as well as being an excellent conductor of both heat and electricity.[15] Compared to nanoclay platelets, GO has much better mechanical properties and a larger specific surface area, which can maximize the interfacial contact between a polymer and the filler, so it has the potential to be an effective reinforcing nanofiller and compatibilizing agent.[18] Most attention has been focused on the preparation of polymer composites filled with various types of graphene-based nanomaterials to enhance their properties.

Cao *et al.*[14] reported the compatibilization effect of immiscible polyamide (PA)/polyphenylene oxide (PPO) (90/10) blends, in which the droplet size of the minor PPO phase was dramatically reduced upon incorporation of only 0.5 wt % GO sheets. They attributed this result to the fact that the GO sheets can interact strongly with both the PA and PPO phases, thus minimizing their interfacial tension. Hence, remarkable increases in the mechanical strength and thermal stability were noted. However, according to the authors, the GO content was relatively high. Paydayesh *et al.*[19] reported the effect of introducing different amounts (1–3 phr) of graphene nanoplatelets on the morphology, mechanical properties, and thermal properties of PLA/poly(methyl methacrylate) (PMMA) blends. The droplet size of the PMMA phase for 3 phr graphene nanoplatelets loading was smaller than that for 1 phr loading, and a more uniform morphology was reported. In the case of PLA/PMMA composite with 1 phr graphene platelets loading, the TEM study revealed that most of the graphene nanoplatelets were selectively located in the PMMA phase, while graphene nanoplatelets were located in both phases in the case of composite with 3 phr graphene nanoplatelets loading. The increments of the thermal stability, tensile modulus, and mechanical strength of the PLA/PMMA/graphene nanoplatelets composites, as well as the reduction of the elongation at break, were found to be directly proportional to the graphene nanoplatelets loading. Chieng *et al.*[20] reported the incorporation of highly exfoliated graphene nanoplatelets to the PLA/epoxidized palm oil (EPO) blend significantly increased the tensile strength and elongation at break, with no effect on the flexural strength and modulus. In addition, the impact strength was reportedly enhanced by the addition of 0.5 wt % graphene nanoplatelets. More recently, Chieng *et al.*[21] demonstrated the nano-reinforcement efficiency of graphene nanoplatelets towards PLA/poly(ethylene glycol) (PEG) composites, the addition of 0.3 wt % graphene nanoplatelets was reported to yield the optimum tensile strength and elongation at break. Therefore, it is clear that researchers have not yet produced polymeric composite materials with balanced properties at low loadings of GO.

In our ongoing study, a series of PLA/PCL blends was prepared and fully characterized to identify the unique PLA/PCL blend system. We then recommended that fillers with high thermal stability should be introduced into the 60PLA/40PCL blend system. This blend ratio was selected because of its balanced mechanical properties and crystallization rate coefficient resulting from the morphology development at 60PLA/40PCL blend (Figure S1, Supporting Information). However, other researchers, such as Wu *et al.*,[22] Jain *et al.*,[23] and Eng *et al.*,[11] proposed different blend ratio which was based on the morphological characteristics and final mechanical and material properties blends after filler incorporation.

On the basis of our search, G particles were selected owing to their high thermal stability and light weight. However, because they have a strong tendency to agglomerate, it is necessary to modify their surface chemistry to improve the wettability with the polymer matrices and study the influences on the properties of the neat PLA/PCL blend. For this purpose, GO is prepared from natural G powder or flakes. If the G is well oxidized, carboxyl, hydroxyl, epoxy, and alkoxy functional groups will be introduced on the surface of most of the GO sheets. This will result in slight exfoliation of the GO, which in turn reduces the number of graphene sheets. These advantages could influence the dispersion of the GO particles in the polymer matrix and enhance various properties of the polymeric composites for various applications. As a result, PLA/PCL composite systems with good properties can probably be obtained at lower GO loadings than would be required for G. In addition, the low loading decreases the difficulty and cost of production of the end product, as well as its total weight.

With this rationale in mind, in this study we have found interesting properties in G- and GO-filled blend composites regime,

which have not been reported before. Few studies have been carried out for PLA/PCL/G composites with a different range of PLA/PCL ratio to the chosen ratio,[24,25] but no comparative studies at very low loading of G and GO as fillers has come to the attention of the authors to date. The compatibilization efficiency and hence reinforcement of very low loadings of G and GO on the morphology, thermal, mechanical, and rheological properties as well as the crystallization behavior of the neat PLA/PCL blend were extensively studied, compared, and discussed in the context of the available literature. Furthermore, the effect, if any, of differences in the surface area of similar particles (G and GO) on the final properties of the PLA/PCL blend composites was analyzed to provide nanoscience and nanotechnology motivation for the first time.

## EXPERIMENTAL

### Materials

Concentrated $H_2SO_4$ (95%–98% purity, $M_W = 98.08$ g mol$^{-1}$, $\rho = 1.840$ g mL$^{-1}$) and HCl ($M_W = 36.46$ g mol$^{-1}$, $\rho = 1.2$ g mL$^{-1}$ at 25 °C, boiling point >100 °C) were purchased from Sigma-Aldrich, South Africa. ACS-reagent-grade $KMnO_4$ (≥99% purity, $M_W = 158.03$ g mol$^{-1}$), $H_2O_2$ (99% purity), acetic acid, G powder, and diethyl ether were also purchased from Sigma-Aldrich, South Africa.

The PLA used in this study was a commercial-grade (PLA U'Z S-17) PLA obtained from Toyota, Japan. It is a low-D PLA with an L-isomer content of >99%, $M_W = 120$–$135$ kg mol$^{-1}$, $\rho = 1.24$ g cm$^{-3}$, a melt flow index of 15.84 g/10 min (190 °C/2.16 kg, according to the ISO 1133B standard method), $T_g = 62$ °C, and $T_m = 175$ °C. PCL was purchased from Sigma-Aldrich, South Africa. According to the supplied information, it has $M_W = 80$ kg mol$^{-1}$, $\rho = 1.145$ g cm$^{-3}$, melt flow index = 5.57 g/10 min (190 °C/2.16 kg, according to the ISO 1133B standard method), and $T_m = 60$ °C. Before use, the PLA was dried at 80 °C and the PCL was dried at 40 °C under vacuum for 12 h.

### Preparation of GO

GO was prepared through chemical oxidation of natural G powder according to the improved Hummers method reported by the Marcano *et al.*[26] Details can be found in the Supporting Information.

### Preparation of Blend and G- and GO-Filled Blend Composites

Neat PLA/PCL (60/40) blend and blend composites containing 0.05 to 0.25 wt % of either G or GO particles were prepared via melt-mixing in a HAAKE PolyLab OS Rheomix (Thermo Electron Co.) batch mixer operated at a rotor speed of 60 rpm and a temperature of 195 °C for 8 min. Prior to melt mixing, all components were dry mixed in a plastic bag. The neat PLA/PCL blend and composites were then compression-molded into different shapes at 195 °C using a Carver 973214 A hot press at 1.2 MPa and cooled to ±20 °C. The prepared samples containing 0, 0.05, 0.1, and 0.25 wt % G or GO particles are denoted blend, blend/0.05 G, blend/0.1 G, blend/0.25 G, blend/0.05GO, blend/0.1GO, and blend/0.25GO, respectively.

### Characterization

X-ray diffraction (XRD) experiments on the compression-molded neat blend and blend composite samples were conducted using an X'Pert PRO diffractometer (PANanalytical, The Netherlands) equipped with Cu-Kα radiation (λ = 1.54 Å), and the samples were scanned at a scan step of about 0.026°. The generator was operated at a voltage of 45 kV and a tube current of 40 mA. The morphologies of the samples were analyzed using field-emission SEM (JSM-7500, JEOL, Japan). The blend and composite samples were first freeze-fractured in liquid nitrogen, and then the PCL minor phase was etched with acetic acid for 15 h at room temperature. The etched fractured surface was then sputter-coated with carbon, and the sides were painted with a silver paste and finally imaged at an acceleration voltage of 3 kV. Thermogravimetric analysis (TGA) of the powder, neat blend, and composite samples was performed using a TG analyzer (model Q500, TA Instruments). Samples weighing about 10 mg were heated in platinum pans from about 30 to 900 °C at a scan rate of 10 °C min$^{-1}$ under flowing nitrogen (20 mL min$^{-1}$). For each type of sample, the experiment was done at least three times, and the most representative result is reported. The thermal properties of the prepared neat blend and composite samples weighing approximately 5.6 mg and placed in aluminum pans were investigated using a differential scanning calorimetry (DSC) (model Q2000, TA Instruments). The samples were heated from −65 to 200 °C at a heating rate of 10 °C min$^{-1}$ under a constant nitrogen flow (25 mL min$^{-1}$) and held for 2 min at 200 °C to erase the thermal history. The samples were then cooled to −65 °C at a cooling rate of 10 °C min$^{-1}$ and heated to 200 °C at a heating rate of 10 °C min$^{-1}$. The second heating results are reported. For each type of sample, analyses were done three times and the average is reported to confirm the quality of results. Equation (1) was used to calculate the degree of crystallinity.

$$\%\ \text{Crystallinity}\ (\%\chi_c) = \frac{\Delta H_m}{\Delta H_m \times W_f} \times 100 \qquad (1)$$

where $\Delta H_m$ is the specific melting enthalpy of each polymer phase in a sample, $W_f$ is the weight fraction of each polymer within the sample, and $\Delta H^\circ_m$ is the specific melting enthalpy of 100% crystalline PLA and PCL, which are 93[3] and 135 (J g$^{-1}$),[27] respectively. The spherulitic growth behavior of the neat blend and composite samples was studied using a polarized optical microscope (POM). Leftovers from the compression-molded thin film samples were placed between two covering glasses and placed on a Linkam hot stage, (Linkam Scientific Instruments Ltd., UK) in the microscope. The samples were heated from room temperature to 200 °C at a heating rate of 10 °C min$^{-1}$, held at 200 °C for 5 min while OM images were taken, and then cooled to 120 °C at the same cooling rate. The samples were held isothermally at 120 °C for 20 min while OM images were taken to study the spherulitic growth behavior of the neat blend and composites. Tensile tests of the compression-molded dog-bone-shaped neat blend and composite samples were conducted using an Instron 5966 tester (Instron Engineering Corp.) with a load cell of 10 kN. The tests were performed to determine the mechanical properties of the samples under tension mode at a single strain rate of 5 mm/min at 30 °C.

Compression molded, dog-bone-shaped specimens approximately 3 mm in thickness, 3.40 mm in width, and 25 mm in gauge length were used. The reported results are an average of at least six independent tensile test measurements. The dynamic mechanical properties of compression molded rectangular samples with dimensions of approximately 12.40, 9.90, and 1.70 mm (length, width, thickness) were studied using a PerkinElmer DMA 8000 analyzer under dual-cantilever bending mode. Analyses were made at various temperatures ranging from −90 to 90 °C at a heating rate of 2 °C $min^{-1}$. Samples were measured at a constant frequency of 1 Hz with a strain amplitude of 0.02%. For each type of sample, two analyses were done to confirm the reproducibility of the results. Melt-state dynamic rheological measurements were made using a Physica MCR501 (Anton Paar, Austria) rheometer equipped with 25-mm diameter parallel plates. Disc-shaped compression molded samples were measured at about 190 °C under nitrogen, with a strain amplitude of 1% and a zero gap of 1.15 mm. The measurements were made using a circular disc approximately 25 mm in diameter and 1.68 mm in thickness. The oscillatory shear at increasing strain amplitude was examined at a fixed frequency of 1 rad $s^{-1}$.

## RESULTS AND DISCUSSION

### Structure and Morphology of G- and GO-Filled Blend Composites

The chemical, structural, and morphological characteristics of the G and GO particles can be found in the Figures S2 and S3, Supporting Information. The dispersion characteristics of G and GO in the melt-processed PLA/PCL blend composites were analyzed using XRD. The XRD patterns of the neat blend and G- and GO-filled blend composites are shown in Figure 1(a,b), respectively. The XRD patterns of neat PLA and PCL are presented in Supporting Information Figure S4. The neat blend is characterized by three significant diffraction peaks. The first peak, at $2\theta = 16.37°$, corresponds to the (110) or (200) reflection plane and is assigned to the PLA matrix. On the other hand, the diffraction peaks appearing at $2\theta = 21.40°$, 21.91°, and 23.66° correspond to the (110), (111), and (200) reflection planes, respectively, and are assigned to the PCL matrix. When G and GO are added to the blend, the intensity of the characteristic PLA diffraction peak increases, and this increase is maximum for the blend composites containing 0.1 wt % G and 0.05 wt % GO. However, the intensity of the diffraction peaks related to PCL remains unchanged. This indicates that G and GO may be present in the PLA matrix and acting as nucleators for the crystallization of the PLA chains. In addition, the characteristic diffraction patterns of G and GO (Figure S2, Supporting Information) did not appear in the XRD patterns of any of the blend composite samples. The reason may be the high-level dispersion and distribution of G and GO within the PLA or blend matrix.[28] However, considerable care should be exercised in reaching this conclusion, because XRD alone is not sufficient to prove dispersion and localization of G and GO in blend composites. Another reason may be the dilution effect, as very small amounts of G and GO are loaded in the blend composites. However, this low G or GO content was sufficient to activate

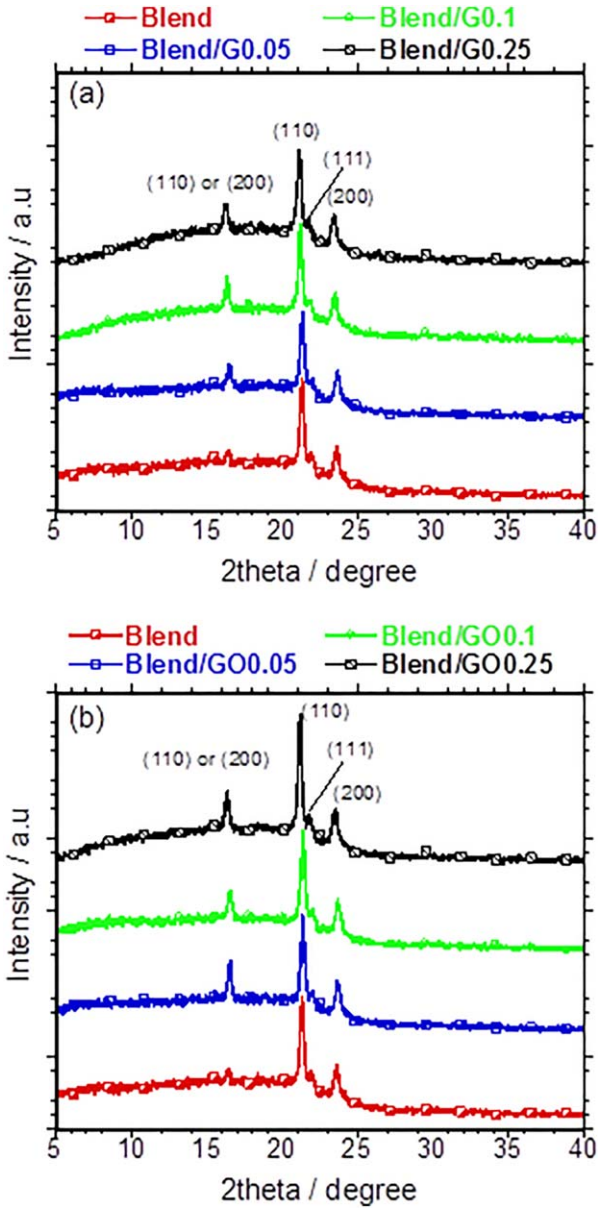


**Figure 1.** X-ray diffraction (XRD) patterns of neat polyamide (PLA)/poly(ε-caprolactone) (PCL) blend and PLA/PCL/G and PLA/PCL/GO composites at various loadings. [Color figure can be viewed at wileyonlinelibrary.com]

crystallization of the PLA matrix, in the blend composite systems.

Figure 2 shows the freeze-fractured surface morphology of the neat blend and G- and GO-filled blend composites, where the dark holes are the etched PCL minor phase. The inset table in Figure 2 shows the number average radius ($R_n$) of the dispersed PCL droplets determined by imageJ software (ImageJ 1.46r), using the following eq. (2).

$$R_n = \frac{\sum n_i R_i}{n_i} \quad (2)$$

where $n_i$ is the number of the dispersed droplets with a radius $R_i$ counted from the SEM images in Figure 2. It is notable that

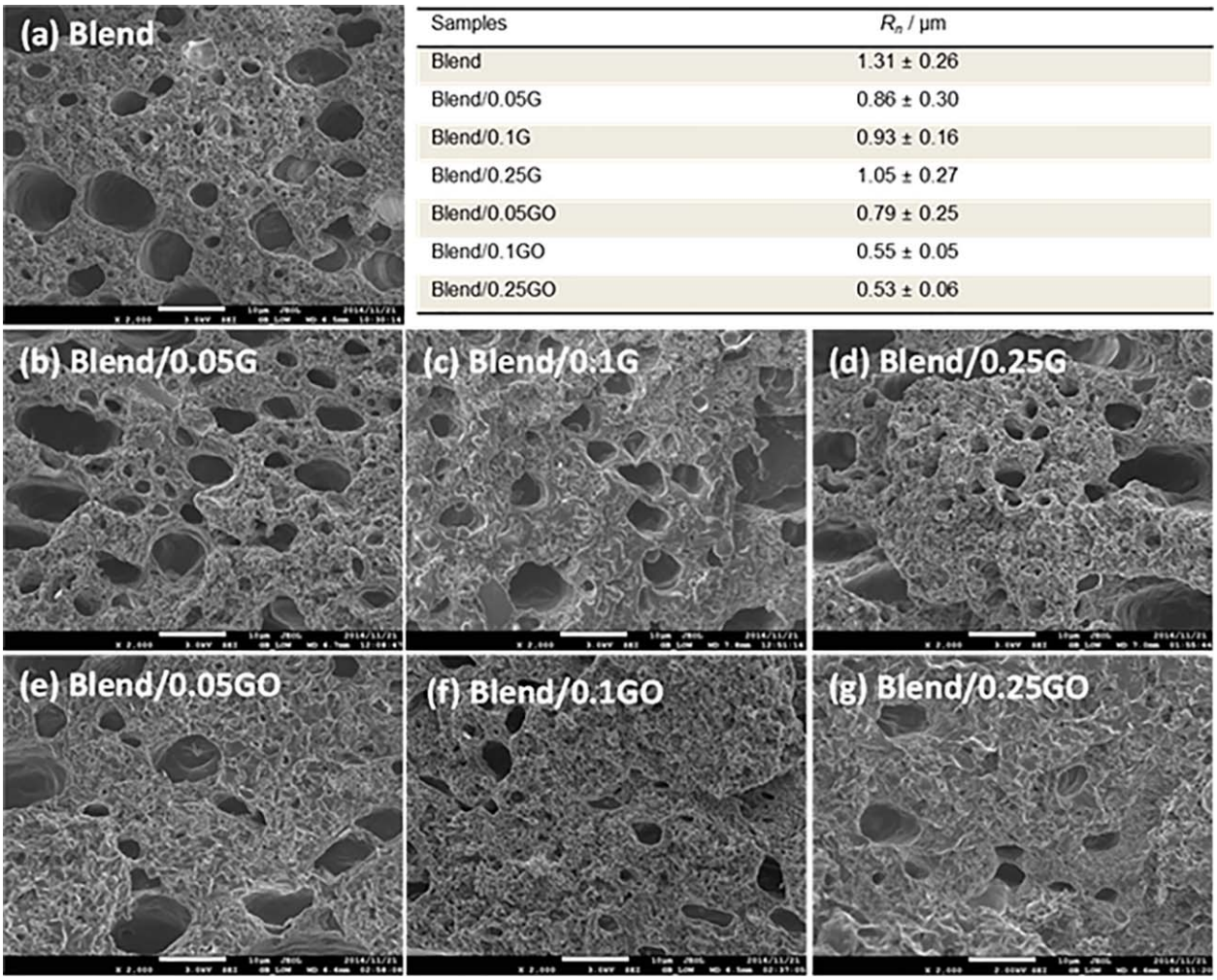


| Samples | $R_n$ / μm |
|---|---|
| Blend | 1.31 ± 0.26 |
| Blend/0.05G | 0.86 ± 0.30 |
| Blend/0.1G | 0.93 ± 0.16 |
| Blend/0.25G | 1.05 ± 0.27 |
| Blend/0.05GO | 0.79 ± 0.25 |
| Blend/0.1GO | 0.55 ± 0.05 |
| Blend/0.25GO | 0.53 ± 0.06 |

**Figure 2.** Freeze-fractured surface morphology of neat polyamide (PLA)/poly(ε-caprolactone) (PCL) blend and PLA/PCL/G and PLA/PCL/GO composites at various loadings, and inset table of the $R_n$ of the dispersed PCL droplets. [Color figure can be viewed at wileyonlinelibrary.com]

all the prepared samples show immiscibility. The neat blend shows PCL droplets of irregular size dispersed within the PLA matrix [Figure 2(a)]. The addition of 0.05 wt % G to the neat blend increases the number of PCL droplets and improves the nonuniformity of the dispersed phase [Figure 2(b)], which may degrade the mechanical properties, as discussed below. The dispersed phase morphology changes slightly with the addition of 0.1 wt % G [Figure 2(c)]. However, the loading of 0.25 wt % G leads to the formation of an elongated, irregular, and nonuniform PCL dispersed phase [Figure 2(d)]. This observation may be the result of agglomeration of G particles in the blend composite [Supporting Information Figures S5(a) and S6(d)].

On the other hand, the GO-filled blend composites show a much finer PCL dispersed phase morphology than the G-filled blend composites [Figure 2(e–g)]. This suggests that GO is better and able to compatibilize the immiscible PLA and PCL blend. It is well known that as the compatibility of immiscible blends improves, the dispersion of the minor phase into the matrix becomes more uniform.[14] It is notable that the addition of 0.25 wt % GO to the PLA/PCL blend leads to the formation of a composite with a very fine dispersed phase morphology [Figure 2(g)], indicating the maximum compatibilization effect of GO for the 60PLA/40PCL blend system. Cao *et al.*[14] reported similar behavior in their study based on the compatibilization of an immiscible PA/PPO blend by the addition of GO. The reduction of PCL droplets in the GO-filled composites is in good agreement with the TGA results, which will be discussed in the following section. However, the observed surface morphology seems inconsistent with the elongation at break for the GO-filled composites. The elongation at break is generally expected to increase when the filler has compatibilization effects, which is not the case in the current study owing to the stiffness of GO. In brief, a moderate decrease of the PCL droplets size is observed with the addition of G and GO particles relative to that of the neat blend. It should be noted that further addition of G particles into the blend (0.1 and 0.25 wt % G particles) increases the size of the PCL droplets relative to the 0.05 wt % G-filled blend composite; however, the attained $R_n$ value are still $<$1.31 μm. In addition, further increase in GO particles loading decreases the size of the PCL droplets even more relative to the 0.05 wt % GO-filled blend composite [inset table in Figure 2].

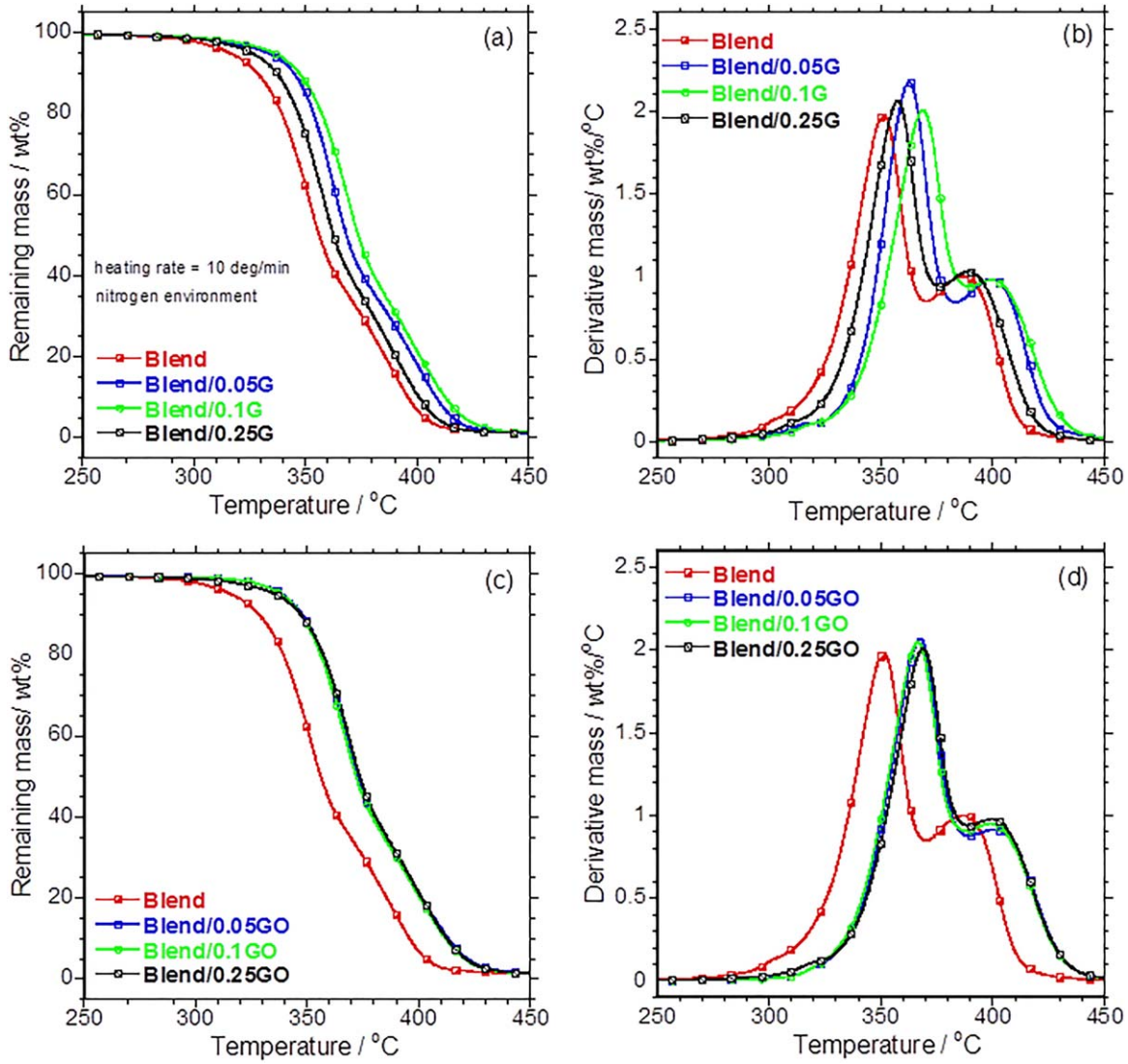


**Figure 3.** Thermogravimetric analysis (TGA) (a) and (c) and derivative (b) and (d) thermograms of neat polyamide (PLA)/poly(ε-caprolactone) (PCL) blend and PLA/PCL/G and PLA/PCL/GO composites at various loadings. [Color figure can be viewed at wileyonlinelibrary.com]

**Effect of G and GO NPs on Thermal Stability of Blends**

TGA curves of the neat blend and its composites with various loadings of G and GO are presented in Figure 3. It is believed that incorporating G or GO particles into a polymeric material can improve its thermal stability.[28] The thermal stability increment of such a polymer composite system is related to either the higher thermal stability of the filler or homogeneous dispersion of the filler in the polymer matrix. Homogeneous dispersion of GO sheets creates a physical protective barrier and delays volatilization of gases, improving the thermal stability. Figure 3 shows that the neat blend is characterized by two-step degradation, indicating that the blend system is immiscible. This is clearly seen in the derivative curves, where the maximum weight loss of the first component occurs at about 364 °C, whereas that of the second component occurs at 398 °C [Figure 3(b,d)]. The incorporation of more thermally stable G particles enhanced the thermal stability of the neat blend [Figure 3(a)]. Briefly, the thermal stability of the neat blend increases with the addition of 0.05 wt % G, increases further with the addition of 0.1 wt % G, which is the optimum loading, and finally decreases with the addition of 0.25 wt % G. The decrease in thermal stability at 0.25 wt % G suggests agglomeration of the G particles in the blend matrix [Supporting Information Figures S5(a) and S6(d)]. For the GO-filled blend, the thermal stability of the neat blend increases [Figure 3(c)].

It is important to note that the addition of more GO does not significantly influence the thermal stability of the blend/0.1GO and blend/0.25GO composites compared to that of the blend/0.05GO composite. This behavior indicates that GO is better dispersed than G in the blend matrix; the reason is the attached carboxyl and hydroxyl functional groups on the edges, top, and bottom of the graphene sheets, which improve the compatibility of the GO particles with the polymer matrices and further form a possible network structure. Thus, a very small amount of GO

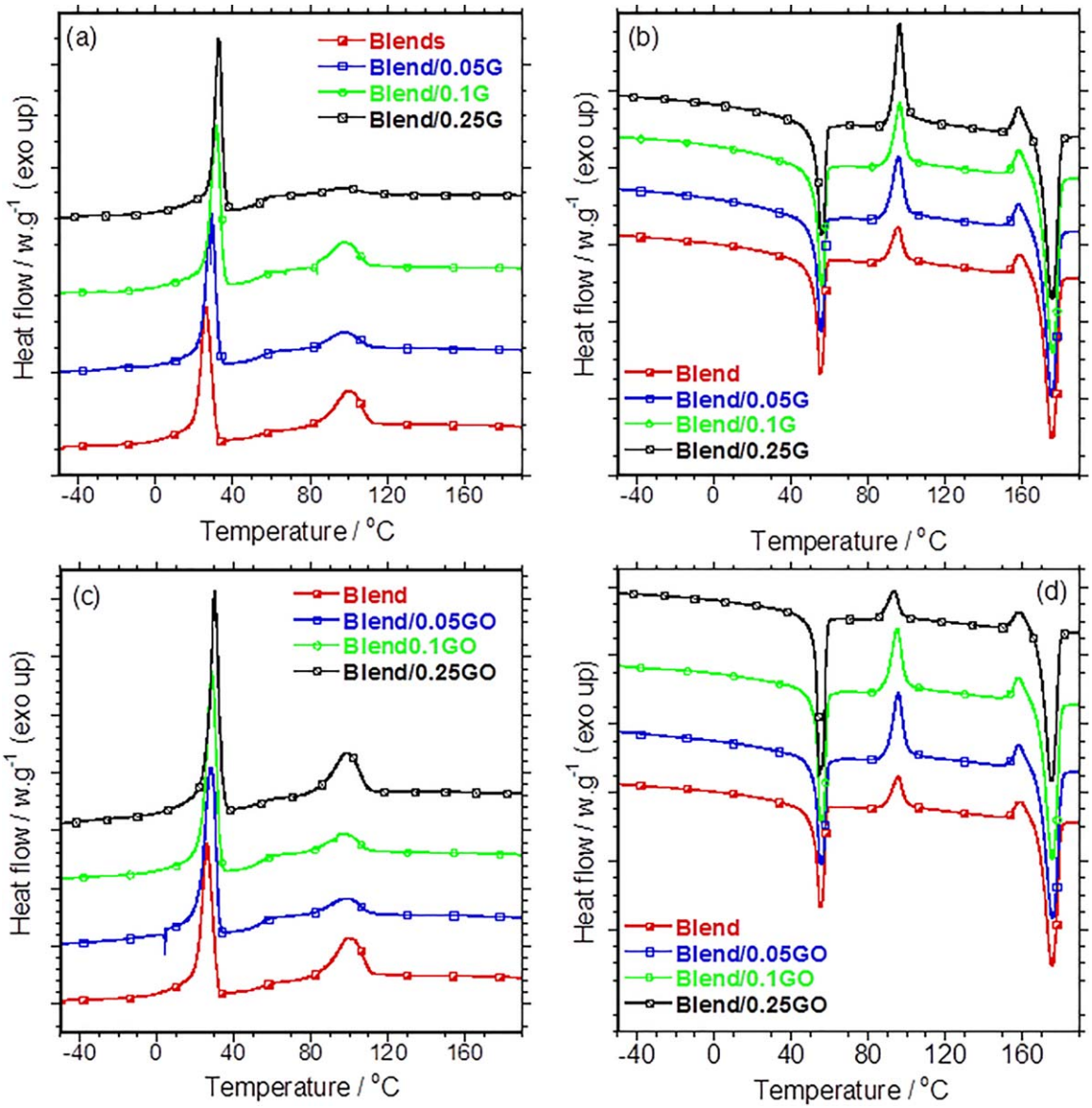


**Figure 4.** Differential scanning calorimetry (DSC) cooling (a) and (c) and heating (b) and (d) thermograms of neat polyamide (PLA)/poly(ε-caprolactone) (PCL) blend and PLA/PCL/G and PLA/PCL/GO composites at various loadings. [Color figure can be viewed at wileyonlinelibrary.com]

can be used instead of a slightly larger amount of G to obtain the same result. In addition, it is interesting to note that GO, which has lower thermal stability than G particles [Supporting Information Figure S2(c)], improves the thermal stability of the neat blend; this behavior fully supports the theoretical indications that particles dispersion and network structural formation are crucial to producing better products for various applications.

**Melting, Crystallization, and Spherulitic Growth Behavior**

The DSC cooling curves presented in Figure 4(a,c) show the crystallization behavior of the neat blend and its G- and GO-filled composites. The DSC thermograms of neat PLA and PCL are presented in Figure S7, Supporting Information. The crystallization temperatures ($T_c$) and crystallization enthalpy ($\Delta H_c$) values obtained from the thermograms are summarized in Table I. The neat blend is characterized by two $T_c$ peaks at 97 and 26 °C, where the former is related to the PLA matrix, and the latter is associated with the PCL minor phase [Figure 4(a or c)]. When G particles are incorporated, the peak position does not change significantly; however, the intensity of the high-temperature $T_c$ peak decreases at a loading of 0.25 wt %. This behavior suggests that the PLA chains folded differently due to the excess amount of G particles and leads to the alteration of the lamellae thickness, hence low intense $T_c$ peak particularly for PLA. Furthermore, the less intense $T_c$ peak [Figure 4(a)] is related to the more intense $T_{cc}$ peak [Figure 4(b)]. It is notable that the $\Delta H_{c(PLA)}$ values of the blend/0.05 G, blend/0.1 G, and blend/0.25 G composites are 5.79, 7.95, and 2.51 J $g^{-1}$, respectively, and these values are lower than that of the neat blend (13.46 J $g^{-1}$). Moreover, the $\Delta H_{c(PCL)}$ values do not change significantly with the incorporation of G filler (Table I). For the

**Table I.** Data Obtained from DSC Cooling and Second Heating Thermograms

| Samples | $T_{cc}$ (°C) | $\Delta H_{cc}$ (J g$^{-1}$) | $T_c$ (°C)[a] | $\Delta H_c$ (J g$^{-1}$)[a] | $T_m$ (°C)[a] | $\Delta H_m$ (J g$^{-1}$)[a] | $X_c$ (%)[a] |
|---|---|---|---|---|---|---|---|
| Neat PLA | 95.87 ± 0.12 | 1.49 ± 0.15 | 101.47 ± 0.16 | 31.40 ± 1.36 | 176.91 ± 0.01 | 55.26 ± 0.32 | 59.42 |
| Neat PCL | – | – | 27.23 ± 0.06 | 64.03 ± 2.43 | 55.48 ± 0.02 | 62.63 ± 1.64 | 46.39 |
| Blend | 96.07 ± 0.15 | 6.11 ± 0.27 | 97.80 ± 0.16 | 13.46 ± 0.56 | 176.42 ± 0.10 | 32.53 ± 0.47 | 58.3 |
| | | | 26.38 ± 0.54 | 22.90 ± 0.33 | 56.13 ± 0.07 | 17.23 ± 0.17 | 31.91 |
| Blend/0.05G | 95.83 ± 0.30 | 14.65 ± 0.44 | 97.69 ± 0.25 | 5.79 ± 0.33 | 175.89 ± 0.28 | 33.90 ± 0.75 | 60.78 |
| | | | 28.79 ± 0.23 | 22.68 ± 0.43 | 55.76 ± 0.30 | 16.64 ± 0.86 | 30.83 |
| Blend/0.1G | 96.81 ± 0.22 | 12.08 ± 0.45 | 97.58 ± 0.07 | 7.95 ± 0.10 | 175.91 ± 0.11 | 33.95 ± 0.02 | 60.9 |
| | | | 30.66 ± 1.26 | 22.62 ± 0.21 | 55.76 ± 0.26 | 17.49 ± 0.33 | 32.42 |
| Blend/0.25G | 96.65 ± 0.08 | 19.62 ± 0.94 | 96.93 ± 0.10 | 2.51 ± 0.44 | 175.72 ± 0.13 | 34.81 ± 1.88 | 62.54 |
| | | | 32.84 ± 0.56 | 23.14 ± 2.01 | 55.99 ± 0.08 | 16.92 ± 0.87 | 31.41 |
| Blend/0.05GO | 95.84 ± 0.02 | 16.23 ± 0.40 | 98.72 ± 0.52 | 5.74 ± 0.43 | 175.91 ± 0.15 | 34.88 ± 0.73 | 62.54 |
| | | | 28.13 ± 0.15 | 25.13 ± 0.74 | 56.03 ± 0.21 | 18.01 ± 0.66 | 33.37 |
| Blend/0.1GO | 95.47 ± 0.21 | 15.18 ± 1.18 | 97.12 ± 0.20 | 6.02 ± 0.37 | 175.99 ± 0.41 | 33.63 ± 0.10 | 60.3 |
| | | | 28.61 ± 0.17 | 26.29 ± 0.88 | 56.23 ± 0.10 | 20.51 ± 0.32 | 38.02 |
| Blend/0.25GO | 92.72 ± 4.43 | 16.23 ± 0.40 | 98.34 ± 0.02 | 12.23 ±0.16 | 175.61 ± 0.21 | 33.71 ± 0.10 | 60.56 |
| | | | 30.17 ± 0.10 | 28.42 ± 0.44 | 55.58 ± 1.14 | 25.81 ± 1.82 | 47.91 |

[a] Top values within the blocks represent PLA temperature profiles; whereas bottom values represent PCL temperature profiles.

blend/0.05GO, blend/0.1GO, and blend/0.25GO composites, the $\Delta H_{c(PLA)}$ values are 5.74, 6.02, and 12.23 J g$^{-1}$, respectively, and these values are also lower than that of the neat blend. However, the $\Delta H_{c(PCL)}$ values are much higher, 25.13, 26.29, and 28.42 J g$^{-1}$, respectively, and exceed that of the neat blend (22.90 J g$^{-1}$) (Table I).

The melting temperature ($T_m$) profiles [Figure 4(b,d)] show no notable changes when either G or GO is incorporated in the composites; however, the total degree of crystallinity ($X_c$) of PLA and PCL in the neat blend is lower than those in the blends with G or GO filler. The $X_c$ value of the G-filled blends shows no significant change; however, a significant change is observed for the composites with GO filler. Importantly, the $X_c$ value of PLA within the composites was not affected as much as that of PCL in the GO-filled blend composites. Briefly, the $X_c$ values of PCL in the blend/0.05GO, blend/0.1GO, and blend/0.25GO composites are 33.37%, 38.02%, and 47.91%, respectively. The dramatic increase resulting from the presence of GO is attributed to the good dispersion of GO particles and the fact that the hydroxyl functional groups on the surface and edges of the single graphene sheets show greater affinity to the PCL minor phase. Furthermore, the significant increment of $X_c$ for PCL suggests a linear increase in the network structural formation of GO particles along the PCL minor phase. However, there is no significant increment for the G-modified blend composites because of the low level of the network filler formation. Low G loading (0.05 and 0.1 wt %) results in fair dispersion, whereas high loading (0.25 wt %) results in agglomeration. On the basis of our knowledge to date, it is not possible to fully correlate the DSC results with the XRD results. However, the small improvement of the $X_c$ values of the PLA matrix in both the G- and GO-filled blend composites supports the assignment of the enhanced diffraction peaks to PLA [Figure 1].

To understand the crystal growth behavior of the neat blend and blend composite samples, POM imaging was performed under isothermal conditions at 120 °C for 20 min. POM images of the neat blend and G- and GO-filled blend composites are shown in Figure 5. The neat blend has a mixture of slightly large and small spherulites, and they are more perfectly grown than those in the G- and GO-filled blend composites; these characteristics influence the tensile properties, as discussed in a later section. It is notable that the spherulites within the neat blend are more densely packed than those of the G- and GO-filled blend composites. It is very hard to differentiate the crystal growth behavior of the G- and GO-filled blend composites. However, it is notable that the PLA spherulites at a loading of 0.05 wt % G are not significantly agglomerated, in contrast to those in all the other composites. In addition, agglomeration of G at a high loading of 0.25 wt % is observable, whereas no agglomeration is observed for GO [Supporting Information Figures S5 and S6(d,g)]. However, increasing the GO loading results in an increased network filler formation, not the significant agglomeration observed for G. This correlates well with the suggestion about agglomeration in the above section. More importantly, the blend with 0.1 and 0.25 wt % GO had smaller dispersed PCL droplets than all the other composites. Both G and GO clearly had greater affinity to the PCL minor phase because most of the G and GO particles are dispersed in the PCL minor phase and at the interface of the PLA/PCL components. These observations reveal that localization of the G and GO fillers in the blend must be considered in order to use them as good nucleating agents in PLA/PCL composites.

### Dynamic Mechanical Properties

Owing to the complexity of the G and GO networks and the nature of the composites, it was practically impossible for the instrument to safely run the 0.05 and 0.1 wt % G- and GO-

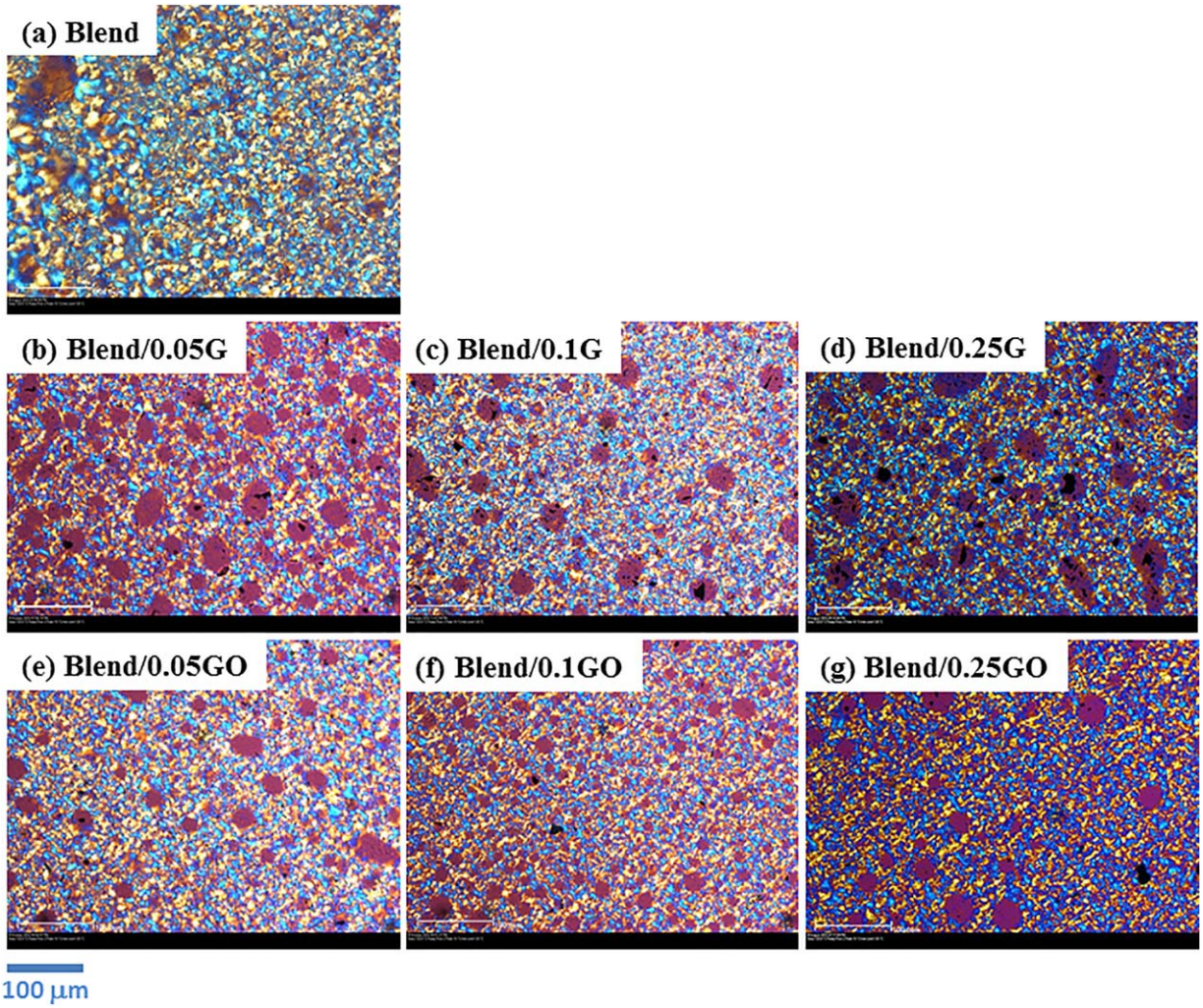


**Figure 5.** Polarized optical microscope (POM) images taken during isothermal melt crystallization at 120 °C for 20 min of neat polyamide (PLA)/poly(ε-caprolactone) (PCL) blend and PLA/PCL/G and PLA/PCL/GO composites at various loadings. Color represents the crystal type within the defined retard waves. Generally, the crystal from the retard light of about 650 nm will be blue, whereas 450 nm will be yellow. [Color figure can be viewed at wileyonlinelibrary.com]

filled blend composite samples. Thus, we attempted to obtain information using the storage modulus ($E'$) and tan δ versus temperature for the 0.25 wt % G and GO-filled blend composites.

Figure 6(a,b) shows the dynamic mechanical properties of the neat blend, blend/0.25 G, and blend/0.25GO composites. The storage modulus of the samples is characterized by three regions, (I), (II), and (III), as seen in Figure 6(a). The storage modulus of the G- and GO-filled composites increases in region (I), unlike that of the neat blend. This suggests that both samples are stiffer than the neat blend, and this result is attributed to the presence of dispersed stiff graphitic particles. Furthermore, in region (I), the moduli of both composites are higher than those in the other regions for the same samples because of the limited chain mobility below region (I). The moduli for both composites in region (II) are still higher than that of the neat blend; however, the modulus of the G-filled composite drops suddenly [region (II)]. The sudden drop suggests a high level of agglomeration of G in the PCL minor phase. Below region (II), the modulus of the G-filled composites increases again, unlike that of the GO-filled composite. Below region (III), the moduli of all the samples drop dramatically; this behavior is attributed to the increased chain mobility of the polymer matrix resulting from the glass transition. Figure 6(b″) clearly indicates an increase in $T_g$ from about 67 to 69 °C ($T_g2$). This supports the observation of a stiffness effect of the G and GO in the surface morphology of the blends. From these observations, it may be concluded that introducing G and GO improved the storage modulus of the PLA/PCL blend system fairly well above and below the $T_g$. However, no significant change is observed in $T_g1$, but the appearance of two different $T_g$ values indicates the immiscibility of the neat blend and composites.

### Tensile Properties

Figure 7(a,b) present the representative stress–strain curves of the neat blend, G- and GO-filled blend composites. The results are summarized in Table II. Notably, when 0.25 wt % G is added to the neat blend, the modulus and tensile strength

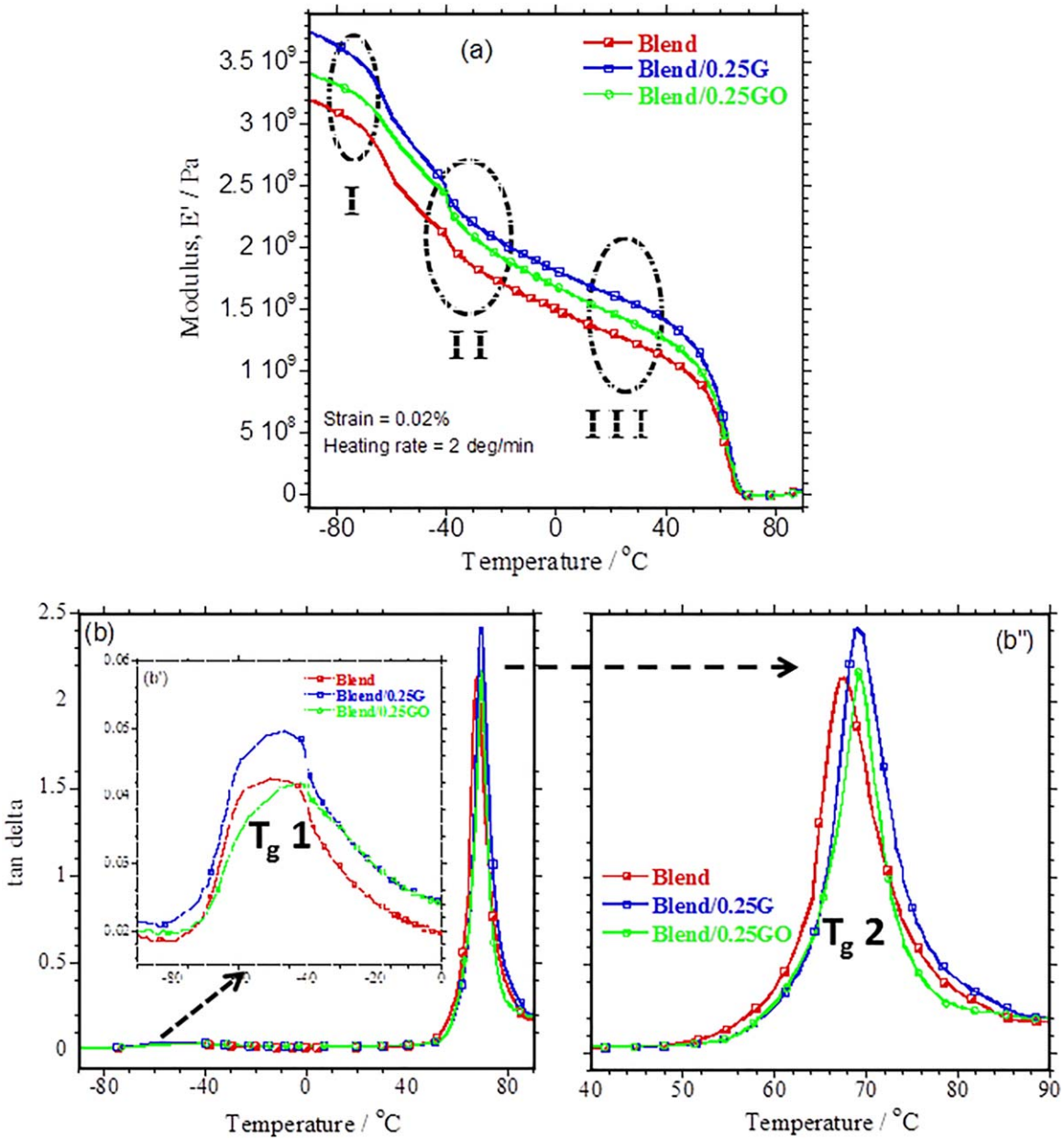


**Figure 6.** Temperature dependence of storage modulus (a) and tan delta (b, b′, and b″) curves of neat polyamide (PLA)/poly(ε-caprolactone) (PCL) blend and PLA/PCL/0.25 G and PLA/PCL/0.25GO composites. [Color figure can be viewed at wileyonlinelibrary.com]

increase by about 1.36% (1987.7 MPa) and 4.80% (68.3 MPa), respectively, compared to those of the unfilled blend (1961.0 MPa and 65.17 MPa). However, the addition of 0.25 wt % GO to the blend decreases the modulus and tensile strength by about 0.54% (1950.5 MPa) and 20.68% (51.69 MPa), respectively, compared to those of the neat blend (Table II). Importantly, the blend/0.25 G composite has better modulus and tensile strength values than the neat blend and GO-filled blend composites. This is an unusual observation in unmodified filler-filled blend composites. However, Natterodt *et al.*[29] reported similar behavior in the case of liner low-density polyethylene/cellulose nanocrystals-2-ureido-4[1 H]pyrimidinone) (LLDPE/CNC-UPy) composites, where LLDPE/CNC-UPy 15% w/w composite showed concurrent improvement in tensile properties. The authors attributed this observation to the formation of intra-CNC rather than inter-CNC UPy dimers in the polymer, and the mobility of the amorphous phase within the polymer matrix. In the current study, G particles demonstrated the possibility of been easily agglomerated in the polymer matrices due to its week wettability as a result of thick graphene sheets [Supporting Information Figure S2(d) and Table S1]. Therefore, the presences of thick graphene sheets prevent particles penetration to the polymer matrices, which results in slight increase in modulus and tensile strength. On the other hand, the addition of small amounts (0.05 and 0.1 wt %) of G and GO dramatically decreases the modulus and tensile strength compared to the unfilled PLA/PCL blend, this behavior suggest the presence of nanovoids within the polymer matrices. However, similar

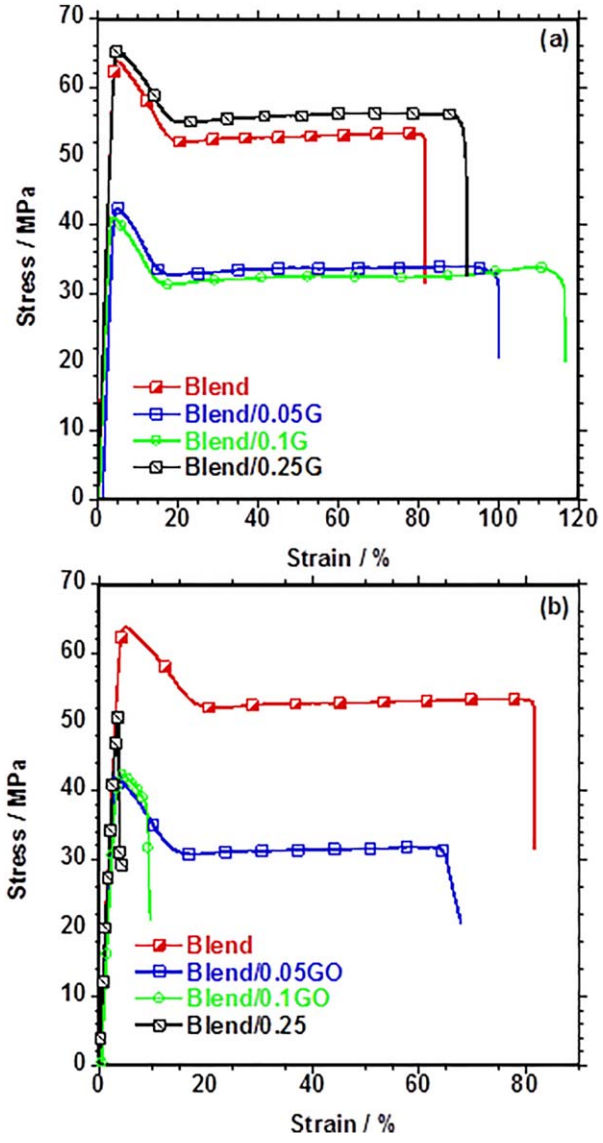


**Figure 7.** Representative stress–strain curves of (a) polyamide (PLA)/poly(ε-caprolactone) (PCL)/G and (b) PLA/PCL/GO composites at various loadings. [Color figure can be viewed at wileyonlinelibrary.com]

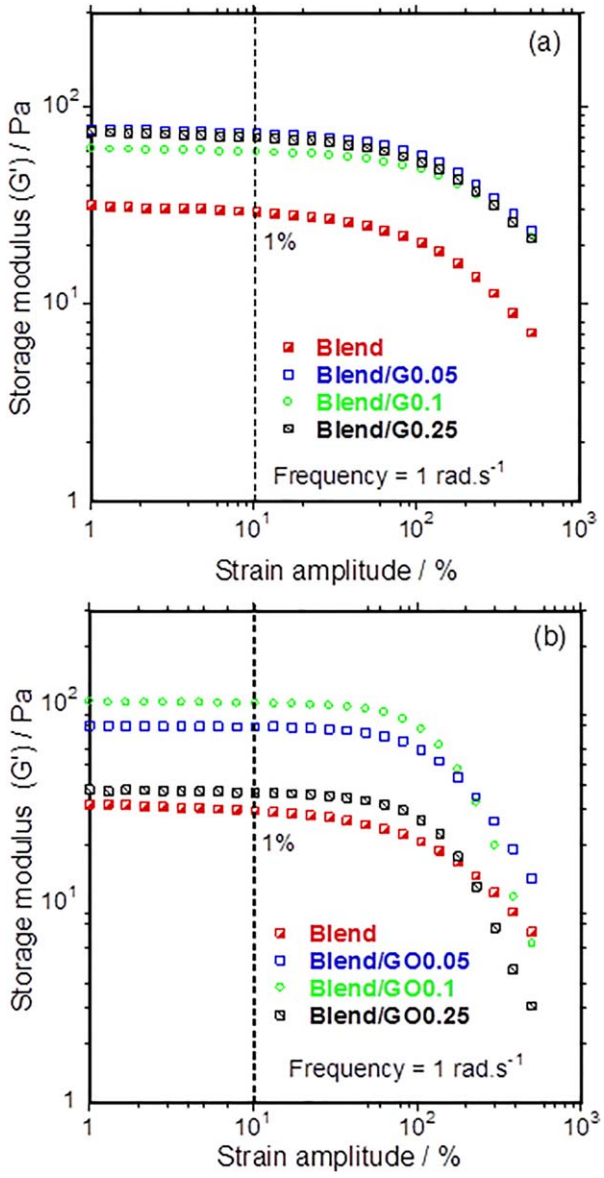


**Figure 8.** Storage modulus versus amplitude of neat polyamide (PLA)/poly(ε-caprolactone) (PCL) blend and PLA/PCL/G and PLA/PCL/GO composites at various loadings. [Color figure can be viewed at wileyonlinelibrary.com]

measured tensile strength values, particularly for lower loading of G- and GO-filled blend composites, have been reported by Forouharshad *et al.*[24]

The blend/0.05 G, blend/0.1 G, and blend/0.25 G composites show elongation at break values of 106.72%, 118.60%, and 110.05%, which are 29.39%, 43.79%, and 33.43% higher,

**Table II.** Tensile Properties of Neat Blend, G-, and GO-Filled Composites at Various Loadings

| Samples | Modulus (MPa) | Tensile strength (MPa) | Elongation at break (%) |
|---|---|---|---|
| Blend | 1961.0 ± 30.20 | 65.170 ± 1.97 | 82.480 ± 7.86 |
| Blend/0.05G | 1757.1 ± 63.76 | 42.080 ± 0.79 | 106.72 ± 5.15 |
| Blend/0.1G | 1511.9 ± 67.04 | 41.180 ± 1.12 | 118.60 ± 3.70 |
| Blend/0.25G | 1987.7 ± 44.24 | 68.300 ± 4.05 | 110.05 ± 9.63 |
| Blend/0.05GO | 1664.2 ± 144.50 | 41.200 ± 0.90 | 69.330 ± 15.00 |
| Blend/0.1GO | 1585.1 ± 65.53 | 39.760 ± 2.60 | 8.3500 ± 2.41 |
| Blend/0.25GO | 1950.5 ± 49.39 | 51.690 ± 2.86 | 4.7200 ± 0.54 |

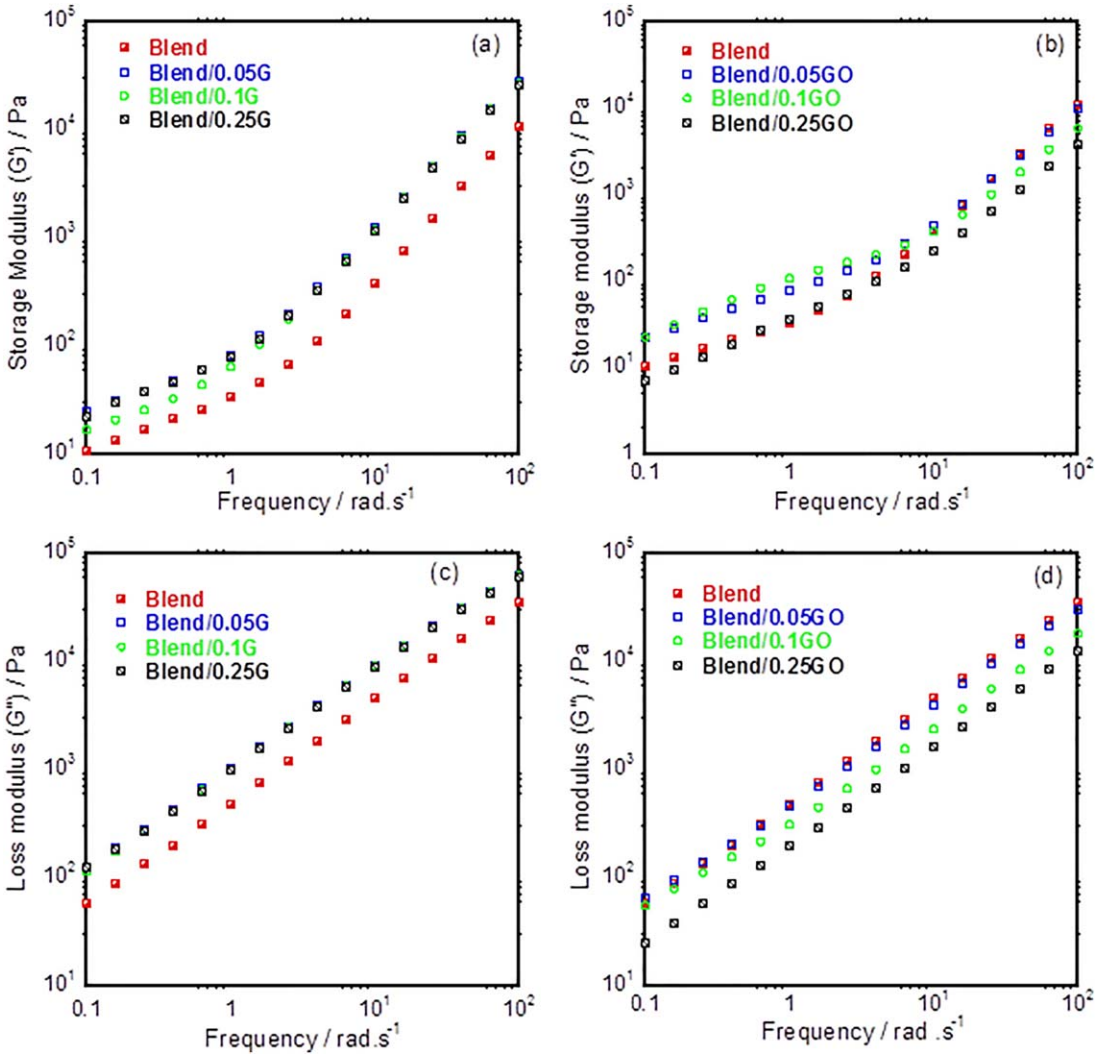


**Figure 9.** Frequency dependence of storage and loss moduli of neat polyamide (PLA)/poly(ε-caprolactone) (PCL) blend and PLA/PCL/G and PLA/PCL/GO composites at various loadings. [Color figure can be viewed at wileyonlinelibrary.com]

respectively, than that of the neat blend (82.48%) (Table II). The reduction in the blend/0.25 G composite is attributed to G agglomeration at high loading, which was observed in the POM images. It is notable that the addition of GO to the PLA/PCL blend made the blend more brittle. Briefly, the blend/0.05GO, blend/0.1GO, and blend/0.25GO composites show decrements of 15.94%, 89.88%, and 94.30%, respectively, in the elongation at break compared to that of the neat blend. This behavior may be attributed to the large aspect ratio of the stiff filler and the interaction between GO and the polymer matrix, which restricts the movement of the polymer chains. Furthermore, the addition of GO particles demonstrated the barrier effects by increasing the thermal stability as discussed earlier, which somehow related to the better dispersion. However, it can be seen that the wettability did not benefit mechanical properties, particularly in the case of GO-filled blend composites. The dispersion effects prevented the diffusion of short polymer chains, hence poor elongation at break or decrease is notable. Other fillers with high aspect ratio, such as CNC in LLDPE system, are reported to enhance modulus and stress with a significant reduction in elongation at break.[30,31] Importantly, the G-filled composites had better elongation at break than the GO-filled composites owing to their fluffy network-like microstructure, which limits the growth of microcracks.

### Melt-State Rheological Properties

To understand the effect of G and GO particles loading on the structural modification of the neat PLA/PCL blend at varying strain amplitudes, strain sweep experiments on neat and G- and GO-filled blend samples were conducted. Figure 8 shows the storage modulus versus amplitude curves of the neat blend and its G- and GO-filled composites. The neat blend shows typical strain softening, suggesting that the PCL droplets were homogenously dispersed in the PLA matrix. However, the addition of G to the blend increases the storage modulus without significantly improving the strain softening behavior, which is consistent with the slight change in the uniformity of the morphology seen in the SEM images above. It is notable that the storage modulus of the blend/0.1 G composite is slightly lower than

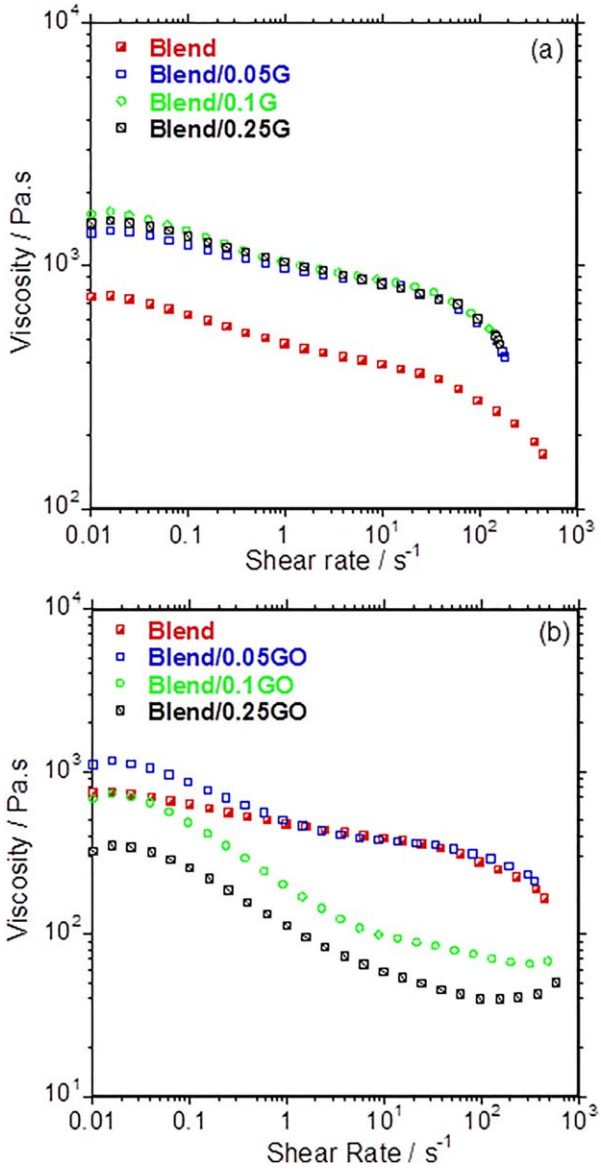


**Figure 10.** Shear viscosity of neat polyamide (PLA)/poly(ε-caprolactone) (PCL) blend and PLA/PCL/G and PLA/PCL/GO composites at various loadings. [Color figure can be viewed at wileyonlinelibrary.com]

those of the blend/0.05 G and blend/0.25 G composites. On the other hand, the addition of GO to the neat blend improves the strain softening of the blend; the addition of 0.05 and 0.1 wt % GO increases the storage modulus, but the addition of 0.25 wt % GO decreases it. The strain softening improvement suggests a more uniform morphology, which was observed earlier in the SEM images, and the decreased storage moduli of the blend/0.25GO composite is consistent with the observed decrease in the tensile properties.

Figure 9 shows the storage ($G'$) and loss moduli ($G''$) versus frequency ($\omega$) curves of the neat blend and G- and GO-filled composites at various loadings. $G'$ is higher for the G-filled blend composites [Figure 9(a)] than for the neat blend. The storage modulus exhibits a noteworthy sudden drop at lower frequencies for the blend/0.1 G composite, but not for the other composites. However, $G''$ increases linearly for all of the G-filled composites [Figure 9(c)] throughout the test. Furthermore, it is notable that there is no change with increasing filler content; this suggests that agglomeration of the fluffy G particles has no significant effect. The blend/0.05GO and blend/0.1GO composites show an increase in $G'$ at lower frequencies compared to the neat blend, whereas at higher frequencies a slight decrease is observed for the blend/0.1GO composite, and $G'$ reaches equilibrium for the blend/0.05GO composite [Figure 9(b)]. The $G'$ degradation at high frequency notable for GO-filled blend composites is attributed to the possible degradation of matrix due to the existence of acid residue in filler particles or network breakdown. These results are similar to that of reported by Salehiyan *et al.*[32] in the PS + C20A/PP blend mixed for 1 min, where the $G'$ decreases at high frequency was notable. In contrast, a decrease in $G'$ is observed for the blend/0.25GO composite. The G″ curves of the GO-filled composites exhibit similar behavior. The moduli reduction is consistent with the observed tensile properties of the GO-filled composites; however, this behavior is attributed to possible network formation of stiff fillers.

Figure 10 shows the viscosity ($\eta^*$) versus shear rate ($\dot{\gamma}$) curves of the neat blend and G- and GO-filled blend composites. The neat blend exhibits non-Newtonian behavior, which results from the blending of two polymers with different viscosity ratios. The addition of G to the neat blend increases the viscosity of the blend [Figure 10(a)]. Importantly, at lower $\dot{\gamma}$, the blend/0.25 G composite shows a slightly reduced viscosity compared to the blend/0.1 G composite. This behavior is consistent with the unusual elongation at break behavior described above. The reduction may be attributed to agglomeration of G particles at a high loading. All of the GO-filled composites exhibit strong non-Newtonian behavior [Figure 10(b)]. In addition, decreasing viscosity is observed for all the GO-filled blend composites; however, a slight upshift at lower $\dot{\gamma}$ is observable for the blend/0.05GO composite. This behavior is consistent with the observed elongation at break behavior of the GO-filled composites, which may be due to the large aspect ratio of the stiff GO particles and leads to brittle composites and hence the low viscosity. Therefore, it is fair to suggest the possible network filler formation within the matrixes as the one of the reasons for the solid-like response of the GO-filled blend composites. It is notable that the G-filled composites had higher zero shear viscosity than the GO-filled composites. On the other hand, at the inertia behavior of 0.1 and 0.25 wt % GO-filled blend composites could be related to the sensitivity of these particular compositions (directly related to observed morphology) at high shear rates. This suggests that the texture of the particles is important in the fabrication of polymer composite materials. This means that softer particles will produce better mechanical properties in the final polymer composite materials, as G is softer than GO.

## CONCLUSIONS

By taking advantage of the high surface area, light weight, few-layered graphene sheet, and unique amphiphilic structure of GO, we prepared GO-filled blend composites with high thermal stability at a low GO loading (0.05 wt %) and a better degree of crystallinity than the neat blend and G-filled composites. However, the addition of more GO further increased the degree of crystallinity

without a notable increase in the thermal stability and agglomeration. On the other hand, a high G content (0.25 wt %) significantly decreased the thermal stability of the prepared composites as a result of agglomeration. With the addition of only 0.05 wt % GO to the immiscible blend, the tensile modulus, tensile strength, and elongation at break decreased slightly compared to those of the neat blend, a trade-off effect of the notable activation of the crystallization process of PLA observed in the XRD results. The addition of more GO worsened the tensile properties but further improved the degree of crystallinity and also activated the crystallization process of the blend system. However, the G-filled composites showed improvements in the tensile properties, such as the elongation at break, compared to the neat blend. The addition of G to the neat blend improved the viscoelastic properties of the neat blend, whereas the addition of only 0.05 wt % GO improved the viscoelastic properties of the neat blend at lower frequencies and maintained the viscoelastic properties of the neat blend throughout the test. On the other hand, the addition of more GO decreased the viscoelastic properties of the neat blend. Furthermore, the addition of GO to the neat blend enhanced the strain softening behavior more than the addition of G did owing to the unique uniformity of the dispersed phase morphology. Considering the inexpensive materials required to prepare GO and the extraordinary properties of GO, this study may open opportunities to produce highly thermally stable GO-filled blend composites at low loadings, which are expected to be of great interest in nanoscience and nanotechnology fields. However, owing to degradation of the mechanical properties of the GO-filled blend composites, it is recommended that the GO be thermally shocked to increase its degree of exfoliation before it is melt-processed with PLA/PCL blend.

## ACKNOWLEDGMENTS

The authors appreciate the financial support of the National Research Foundation, South Africa, together with the University of Johannesburg, and further thank the staff of the Council for Scientific and Industrial Research's NCNSM characterization facility for their work on characterization.

## REFERENCES

1. Peelman, N.; Ragaert, P.; Meulenaer, B. D.; Adons, D.; Peeters, R.; Cardon, L.; Impe, F. V.; Devlieghere, F. *Trends Food Sci. Technol.* **2013**, *32*, 128.
2. Lemmouchi, Y.; Murariu, M.; Santos, A. M.; Amass, A. J.; Schacht, E.; Dubois, P. *Eur. Polym. J.* **2009**, *45*, 2839.
3. Ramontja, J.; Ray, S. S.; Pillai, S. K.; Luyt, A. S. *Macromol. Mater. Eng.* **2009**, *249*, 839.
4. Ojijo, V.; Ray, S. S.; Sadiku, R. *ACS Appl. Mater. Interfaces* **2012**, *4*, 2395.
5. Xu, Z.; Zhang, Y.; Wang, Z.; Sun, N.; Li, H. *ACS Appl. Mater. Interfaces* **2011**, *3*, 4858.
6. Baudoin, A.-C.; Auhl, D.; Tao, F.; Devaux, J.; Bailly, C. *Polymer* **2011**, *52*, 149.
7. Haider, S.; Kausar, A.; Muhammad, B. *Polym. Plast. Technol. Eng.* **2016**, *55*, 1536.
8. Ray, S. S.; Bousmina, M. *Macromol. Rapid Commun.* **2005**, *26*, 450.
9. Wu, B. L.; Wang, J.; He, X.; Zhang, T.; Sun, H. *Package Technol. Sci.* **2014**, *27*, 693.
10. Mofokeng, J. P.; Luyt, A. S. *Polym. Test.* **2015**, *45*, 93.
11. Eng, C. C.; Ibrahim, N. A.; Zainuddin, N.; Ariffin, H.; Zin, W.; Yunus, W.; Then, Y. Y.; Teh, C. C. *Indian J. Mater. Sci.* **2013**. Doi: 10.1155/2013/816503.
12. Liang, J. Z.; Duan, D. R.; Tang, C. Y.; Tsui, C. P.; Chen, D. Z. *Polym. Test.* **2013**, *32*, 617.
13. Agwuncha, S. C.; Ray, S. S.; Jayaramudu, J.; Khoathane, C.; Sadiku, R. *Macromol. Mater. Eng.* **2015**, *300*, 31.
14. Cao, Y.; Zhang, J.; Feng, J.; Wu, P. *ACS Nano* **2011**, *5*, 5920.
15. Georgakilas, V.; Otyepka, M.; Bourlinos, A. B.; Chandra, V.; Kim, N.; Kemp, K. C.; Hobza, P.; Zboril, R.; Kim, K. S. *Chem. Rev.* **2012**, *112*, 6156.
16. Cote, L. J.; Kim, J.; Tung, V. C.; Luo, J.; Kim, F.; Huang, J. *Pure Appl. Chem.* **2011**, *83*, 95.
17. Yang, J.; Feng, C.; Dai, J.; Zhang, N.; Huang, T.; Wang, Y. *Polym. Int.* **2013**, *62*, 1085.
18. Yan, N.; Xia, H.; Wu, J.; Zhan, Y.; Fei, G.; Chen, C. *J. Appl. Polym. Sci.* **2013**, *127*, 933.
19. Paydayesh, A.; Azar, A. A.; Arani, A. J.; Kabir, A.; Campus, M. *Ciência eNatura, Santa Maria.* **2015**, *37*, 15.
20. Chieng, B. W.; Ibrahim, N. A.; Zin, W.; Yunus, W. *Indian J. Mater. Sci.* **2012**, *13*, 10920.
21. Chieng, B. W.; Ibrahim, N. A.; Zin, W.; Yunus, W.; Hussein, M. Z. *Polymer* **2014**, *6*, 93.
22. Wu, D.; Zhang, Y.; Zhang, M.; Yu, W. *Biomacromolecules* **2009**, *10*, 417.
23. Jain, S.; Reddy, M. M.; Mohanty, A. K.; Misra, M.; Ghosh, A. *Macromol. Mater. Eng.* **2010**, *295*, 750.
24. Forouharshad, M.; Gardella, L.; Furfaro, D.; Galimberti, M.; Monticelli, O. *Eur. Polym. J.* **2015**, *70*, 28.
25. Kelnar, I.; Kratochv, J.; Forteln, I.; Kaprlkov, L.; Zhigunov, A.; Nevoralov, M. *Polym. Compos.* **2017**. DOI: 10.1002/pc.24322.
26. Marcano, D. C.; Kosynkin, D. V.; Berlin, J. M.; Sinitskii, A.; Sun, Z.; Slesarev, A.; Alemany, L. B.; Lu, W.; Tour, J. M. *ACS Nano* **2010**, *4*, 4806.
27. Gupta, K. K.; Pal, N.; Mishra, P. K.; Srivastava, P. *J. Biomed. Mater. Res. A* **2014**, *102*, 2600.
28. Milani, M. A.; González, D.; Quijada, R.; Basso, N. R. S.; Cerrada, M. L.; Azambuja, D. S.; Galland, G. B. *Compos. Sci. Technol.* **2013**, *84*, 1.
29. Natterodt, J. C.; Sapkota, J.; Foster, E. J.; Weder, C. *Biomacromolecules* **2017**, *18*, 517.
30. Sapkota, J.; Natterodt, J. C.; Shirole, A.; Foster, E. J.; Weder, C. *Macromol. Mater. Eng.* **2017**, *302*, 1600300.doi:10.1002/mame.201600300.
31. Sapkota, J.; Jorfi, M.; Weder, C.; Foster, E. J. *Macromol. Rapid Commun.* **2014**, *35*, 1747.
32. Salehiyan, R.; Choi, W. J.; Lee, J. H.; Hyun, K. *Korean Aust. Rheol. J.* **2014**, *26*, 311.